Inorganic Chemistry

ARTICLE

pubs.acs.org/IC

Synthetic Entry into Polynuclear Bismuth−Manganese Chemistry: High Oxidation State $Bi^{III}_2Mn^{IV}_6$ and $Bi^{III}Mn^{III}_{10}$ Complexes

Theocharis C. Stamatatos, Katie Oliver, Khalil A. Abboud, and George Christou*

Department of Chemistry, University of Florida, Gainesville, Florida 32611-7200, United States

Supporting Information

ABSTRACT: The first high nuclearity, mixed-metal Bi^{III}/Mn^{IV} and Bi^{III}/Mn^{III} complexes are reported. The former complexes are $[Bi_2Mn^{IV}_6O_9(O_2CEt)_9(HO_2CEt)(NO_3)_3]$ (**1**) and $[Bi_2Mn^{IV}_6O_9(O_2CPh)_9(HO_2CPh)(NO_3)_3]$ (**2**) and were obtained from the comproportionation reaction between $Mn(O_2CR)_2$ and MnO_4^- in a 10:3 ratio in the presence of $Bi(NO_3)_3$ (3 equiv) in either a $H_2O/EtCO_2H$ (**1**) or $MeCN/PhCO_2H$ (**2**) solvent medium. The same reaction that gives **2**, but with $Bi(O_2CMe)_3$ and $MeNO_2$ in place of $Bi(NO_3)_3$ and MeCN, gave the lower oxidation state product $[BiMn^{III}_{10}O_8(O_2CPh)_{17}(HO_2CPh)(H_2O)]$ (**3**). Complexes **1** and **2** are near-isostructural and possess an unusual and high symmetry core topology consisting of a Mn^{IV}_6 wheel with two central Bi^{III} atoms capping the wheel on each side. In contrast, the $[BiMn^{III}_{10}O_8]^{17+}$ core of **3** is low symmetry, comprising a $[BiMn_3(\mu_3\text{-}O)_2]^{8+}$ butterfly unit, four $[BiMn_3(\mu_4\text{-}O)]^{10+}$ tetrahedra, and two $[BiMn_2(\mu_3\text{-}O)]^{7+}$ triangles all fused together by sharing common Mn and Bi vertices. Variable-temperature, solid-state dc and ac magnetization data on **1**−**3** in the 1.8−300 K range revealed that **1** and **2** possess an $S = 0$ ground state spin, whereas **3** possesses an $S = 2$ ground state. The work offers the possibility of access to molecular analogs of the multifunctional Bi/Mn/O solids that are of such great interest in materials science.

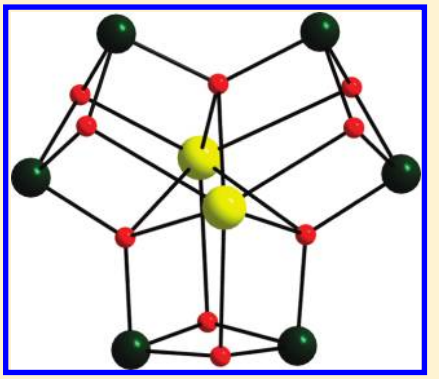

INTRODUCTION

Both discrete and polymeric oxide-bridged compounds of Mn or Bi are of relevance to a large number of areas and applications spanning inorganic, biological, materials, and industrial chemistry, as well as to the multidisciplinary fields of magnetism and electronics.[1] In a biological context, for example, a high oxidation state Mn_4Ca cluster within the photosynthetic apparatus of plants and cyanobacteria is the oxygen-evolving complex (OEC) that catalyzes the oxidation of H_2O to O_2 and is thus the source of essentially all this gas on the planet.[2] This has stimulated extensive efforts to prepare structural and functional model compounds of the OEC, and a large number of Mn_4 molecular complexes have been obtained as a result.[3] Similarly, polyoxidobismuth species play an important role as pharmaceuticals owing to their relatively low toxicity compared with related species containing other heavy metals such as Hg, Cd, Sn, or Pd,[4] and this has stimulated the synthesis of $\{Bi_xO_y\}$ clusters that mimic on a molecular basis the biological properties of the amorphous, polymeric bismuth oxides.[5] In the magnetism arena, one area of molecular manganese chemistry that has attracted much attention is that of high-spin molecules and single-molecule magnets, both arising from the fact that Mn^{III}-containing clusters often possess large, and sometimes abnormally large, ground-state spin (S) values.[6] When this is combined with a large and negative magnetoanisotropy (as reflected in a large and negative zero-field splitting parameter, D), single-molecule magnets (SMMs) result,[7,8] which represent a molecular approach to nanoscale magnetic materials. In addition, they display quantum effects such as quantum tunneling of the magnetization[9] and quantum phase interference,[10] offering the potential for use in molecule-based information storage and molecular spintronics,[11] as well as quantum information processing.[12]

In contrast, Bi compounds are diamagnetic, and the areas of greatest potential are thus not magnetism but, for example, applications of nanoparticles of Bi_2O_3 within sensors and solid electrolytes.[13] However, much more technologically important is the broad spectrum of potential applications offered by the variety of heterometallic Bi-containing metal oxides, which have impacted many areas such as sensors, oxidation catalysts, superconductors, photocatalysts, and next-generation data storage materials.[14] A field of great importance is the class of mixed-metal oxide multiferroics,[15] which are materials simultaneously showing ferromagnetic, ferroelectric, and/or ferroelastic long-range ordering. For example, coupling between the ferroelectric and the magnetic order parameters can lead to intriguing magnetoelectrical effects. Bismuth-containing oxides such as $BiMnO_3$ with a perovskite structure and $BiMn_2O_5$ have been the focus of recent attention due to their potential to act as multiferroic materials exhibiting mutually ferromagnetism and ferroelectricity, thus leading to exciting multifunctional materials.[15,16]

Given the above, it is perhaps surprising that there has been no development of Bi^{III}/Mn^{III}, Bi^{III}/Mn^{IV}, and/or $Bi^{III}/Mn^{III/IV}$ molecular cluster chemistry, only a trinuclear $Bi^{III}_2Mn^{II}$ complex

Received: March 30, 2011
Published: April 26, 2011

having been reported.[17] Diamagnetic Bi^{III} obviously brings no magnetic advantage, and Bi/Mn chemistry has therefore not attracted interest, in contrast to the spin and anisotropy considerations that have made mixed Ln/Mn (Ln = lanthanide) compounds so attractive to many groups during the past several years.[18] Nevertheless, the mixed-metal oxides made us believe that oxide-bridged Bi/Mn molecular species might exhibit interesting new structures related to those of the mixed-metal oxides, and/or properties distinct from those of homometallic Mn or heterometallic Ln/Mn clusters. We have therefore initiated a new program seeking the development of synthetic methods to Bi/Mn molecular species, and we now report the first compounds from this work. We herein describe the synthesis and crystallographic and magnetic characterization of $Bi^{III}{}_2Mn^{IV}{}_6$ and $Bi^{III}Mn^{III}{}_{10}$ clusters. They are the first high-nuclearity, heteronuclear Bi/Mn complexes of any type and have been prepared by a comproportionation route under acidic conditions in the presence of carboxylate ligands, which are widely employed ligand types in both Mn and Bi homometallic cluster chemistry.[19]

EXPERIMENTAL SECTION

Syntheses. All manipulations were performed under aerobic conditions using chemicals and solvents as received, unless otherwise stated. $Mn(O_2CEt)_2 \cdot xH_2O$,[20] $Mn(O_2CPh)_2 \cdot 2H_2O$,[21] and $N^nBu_4MnO_4$[22] were prepared as described elsewhere. ***Warning!*** *Appropriate care should be taken in the use of $N^nBu_4MnO_4$, and readers are referred to the detailed warning given elsewhere.*[22]

$[Bi_2Mn_6O_9(O_2CEt)_9(HO_2CEt)(NO_3)_3]$ (1). To a stirred colorless solution of $Mn(O_2CEt)_2 \cdot xH_2O$ (0.40 g, 2.0 mmol) in $H_2O/EtCO_2H$ (15/3 mL) was added solid $Bi(NO_3)_3 \cdot 5H_2O$ (0.97 g, 2.0 mmol). The resulting white suspension was stirred for a total of 20 min, during which time solid $N^nBu_4MnO_4$ (0.22 g, 0.6 mmol) was added in small portions, causing a rapid color change to dark brown. The final dark brown slurry was filtered and the filtrate left undisturbed to concentrate slowly by evaporation. After 10 days, X-ray-quality dark-brown plate-like crystals of **1** had appeared and were collected by filtration, washed with cold H_2O (2 × 2 mL) and Me_2CO (2 × 5 mL), and dried under a vacuum; the yield was 10%. Anal. Calcd for **1**: C, 19.91; H, 2.84; N, 2.32%. Found: C, 20.15; H, 3.02; N, 2.24%. Selected IR data (cm^{-1}): 3213 (mb), 2965 (m), 1535 (s), 1390 (vs), 1361 (m), 1300 (m), 1272 (m), 1235 (m), 1198 (m), 1047 (m), 966 (m), 934 (m), 906 (m), 806 (m), 772 (w), 733 (s), 639 (m), 606 (s), 579 (m), 519 (w), 475 (m), 449 (w), 416 (w).

$[Bi_2Mn_6O_9(O_2CPh)_9(HO_2CPh)(NO_3)_3]$ (2). Solid $PhCO_2H$ (2.00 g, 16.4 mmol) was dissolved in hot MeCN (50 mL) with stirring, and the resulting colorless solution was treated with solid $Mn(O_2CPh)_2 \cdot 2H_2O$ (0.67 g, 2.0 mmol) and $Bi(NO_3)_3 \cdot 5H_2O$ (0.97 g, 2.0 mmol), which caused a color change to orange. The solution was stirred at 70 °C for a total of 10 min, during which time solid $N^nBu_4MnO_4$ (0.22 g, 0.6 mmol) was added in small portions. The resulting dark brown slurry was allowed to cool down at room temperature, filtered, and the filtrate layered with CH_2Cl_2 (50 mL). After five days, X-ray-quality dark-brown plate-like crystals of $2 \cdot 4MeCN \cdot 2CH_2Cl_2$ had appeared and were collected by filtration, washed with MeCN (2 × 5 mL) and CH_2Cl_2 (2 × 5 mL), and dried under a vacuum; the yield was 30%. Anal. Calcd for **2** (solvent-free): C, 35.06; H, 2.32; N, 2.07%. Found: C, 35.15; H, 2.04; N, 2.34%. The crystal structure shows a 60:40% disorder of a carboxylate with a nitrate (vide infra), and this has been taken into account in the calculation of the expected elemental percentages. Selected IR data (cm^{-1}): 3380 (mb), 1642 (m), 1596 (m), 1532 (s), 1491 (m), 1394 (vs), 1178 (m), 1069 (w), 1025 (m), 1000 (w), 937 (w), 858 (w), 825 (w), 717 (s), 688 (s), 634 (s), 611 (s), 523 (m), 444 (w), 416 (w).

$[BiMn_{10}O_8(O_2CPh)_{17}(HO_2CPh)(H_2O)]$ (3). Solid $PhCO_2H$ (2.00 g, 16.4 mmol) was dissolved in hot $MeNO_2$ (50 mL) with stirring, and the resulting colorless solution was treated with solid $Mn(O_2CPh)_2 \cdot 2H_2O$ (0.67 g, 2.0 mmol) and $Bi(O_2CMe)_3$ (0.77 g, 2.0 mmol), which caused a color change to orange. The solution was stirred at 80 °C for a total of 10 min, during which time solid $N^nBu_4MnO_4$ (0.22 g, 0.6 mmol) was added in small portions. The resulting dark brown slurry was filtered and the filtrate left undisturbed to concentrate slowly by evaporation. After four days, X-ray-quality brown needle-like crystals of $3 \cdot 6PhCO_2H$ had appeared and were collected by filtration, washed with $MeNO_2$ (2 × 3 mL) and CH_2Cl_2 (2 × 5 mL), and dried under a vacuum; the yield was 60%. Anal. Calcd for $3 \cdot 6PhCO_2H$: C, 52.85; H, 3.41%. Found: C, 53.04; H, 3.65%. Selected IR data (cm^{-1}): 3380 (wb), 3063 (m), 2655 (w), 2544 (w), 1966 (w), 1915 (w), 1820 (w), 1690 (s), 1599 (vs), 1533 (sb), 1426 (sb), 1176 (s), 1069 (m), 1025 (m), 1001 (w), 938 (w), 841 (w), 816 (w), 721 (s), 683 (s), 634 (sb), 508 (m), 438 (w), 415 (w).

X-Ray Crystallography. Data were collected on a Siemens SMART PLATFORM equipped with a CCD area detector and a graphite monochromator utilizing Mo Kα radiation (λ = 0.71073 Å). Suitable crystals of **1**, $2 \cdot 4MeCN \cdot 2CH_2Cl_2$, and $3 \cdot 6PhCO_2H$ were attached to glass fibers using silicone grease and transferred to a goniostat where they were cooled to 173 K for data collection. An initial search for reciprocal space revealed a monoclinic cell for **1** and $3 \cdot 6PhCO_2H$ and a tetragonal cell for $2 \cdot 4MeCN \cdot 2CH_2Cl_2$; space groups $P2_1/n$ (**1**), $P\bar{4}2_1/c$ ($2 \cdot 4MeCN \cdot 2CH_2Cl_2$), and $P2_1/c$ ($3 \cdot 6PhCO_2H$) were confirmed by the subsequent solution and refinement of the structures. Cell parameters were refined using up to 8192 reflections. A full sphere of data (1850 frames) was collected using the ω-scan method (0.3° frame width). The first 50 frames were remeasured at the end of data collection to monitor instrument and crystal stability (maximum correction on I was <1%). Absorption corrections by integration were applied on the basis of measured indexed crystal faces. The structures were solved by direct methods in *SHELXTL6*[23] and refined on F^2 using full-matrix least squares. The non-H atoms were treated anisotropically, whereas the H atoms were placed in calculated, ideal positions and refined as riding on their respective C atoms.

For **1**, the asymmetric unit consists of the complete Bi_2Mn_6 cluster and no solvent molecules of crystallization. The hydrogen atom H38 involved in the O38···H38···O8 hydrogen bond was observed in a difference Fourier map and refined as riding on its parent atom. A total of 712 parameters were included in the structure refinement using 9489 reflections with $I > 2\sigma(I)$ to yield an R1 and wR2 of 3.32 and 7.22%, respectively.

For $2 \cdot 4MeCN \cdot 2CH_2Cl_2$, the asymmetric unit consists of the complete Bi_2Mn_6 cluster, and four MeCN and two CH_2Cl_2 molecules of crystallization. The solvent molecules are disordered and could not be modeled properly, thus the program SQUEEZE,[24] a part of the PLATON package of crystallographic software, was used to calculate the solvent disorder area and remove its contribution to the overall intensity data. One Ph ring was disordered at two positions with 50:50% refined occupancies. Another disorder involved a benzoate and a nitrate group at the same site with 60:40% occupancies, respectively. A total of 626 parameters were refined using 9216 reflections with $I > 2\sigma(I)$ to yield an R1 and wR2 of 7.40 and 15.40%, respectively.

For $3 \cdot 6PhCO_2H$, the asymmetric unit consists of the complete $BiMn_{10}$ cluster and six $PhCO_2H$ lattice molecules. The latter could not be modeled properly; thus the program SQUEEZE was again used to calculate the solvent disorder area and remove its contribution to the overall intensity data. The total number of electrons per asymmetric unit was calculated to be 435. This number and the difference Fourier map leads to an estimate of six $PhCO_2H$ lattice molecules. Additionally, one phenyl group was disordered and refined in two parts with 61:39% occupancies. A total of 1598 parameters were included in the final cycle of refinement using 8379 reflections with $I > 2\sigma(I)$ to yield an R1 and wR2 of 6.57 and 16.30%, respectively.

dx.doi.org/10.1021/ic200656q |*Inorg. Chem.* 2011, 50, 5272–5282

Table 1. Crystallographic Data for 1, 2·4MeCN·2CH_2Cl_2, and 3·6$PhCO_2H$

parameter	1	2	3
formula[a]	$C_{30}H_{51}N_3O_{38}Mn_6Bi_2$	$C_{77.2}H_{69}N_{7.4}O_{40.4}Cl_4Mn_6Bi_2$	$C_{168}H_{128}O_{57}Mn_{10}Bi$
fw, g mol^{-1}[a]	1809.34	2593.25	3817.08
cryst syst	monoclinic	tetragonal	monoclinic
space group	$P2_1/n$	$P\bar{4}2_1/c$	$P2_1/c$
a, Å	12.5042(14)	26.2209(15)	16.8942(14)
b, Å	23.884(3)	26.2209(15)	25.356(2)
c, Å	17.900(2)	26.591(3)	35.234(3)
β, deg	94.770(2)	90	92.064(2)
V, $Å^3$	5327.4(10)	18282(3)	15083(2)
Z	4	8	4
T, K	173(2)	173(2)	173(2)
radiation, Å[b]	0.71073	0.71073	0.71073
ρ_{calc}, g cm^{-3}	2.256	1.884	1.681
μ, mm^{-1}	8.063	4.846	2.065
R1[c,d]	0.0332	0.0740	0.0657
wR2[e]	0.0722	0.1540	0.1630

[a] Including solvate molecules. [b] Graphite monochromator. [c] $I > 2\sigma(I)$. [d] $R1 = \Sigma(||F_o| - |F_c||)/\Sigma|F_o|$. [e] $wR2 = [\Sigma[w(F_o^2 - F_c^2)^2]/\Sigma[w(F_o^2)^2]]^{1/2}$, $w = 1/[\sigma^2(F_o^2) + [(ap)^2 + bp]$, where $p = [\max(F_o^2, 0) + 2F_c^2]/3$.

Unit cell data and structure refinement details for the complexes are collected in Table 1.

Physical Measurements. Infrared spectra were recorded in the solid state (KBr pellets) on a Nicolet Nexus 670 FTIR spectrometer in the 400−4000 cm^{-1} range. Elemental analyses (C, H, and N) were performed on a Perkin-Elmer 2400 Series II Analyzer. Variable-temperature dc and ac magnetic susceptibility data were collected at the University of Florida using a Quantum Design MPMS-XL SQUID susceptometer equipped with a 7 T magnet and operating in the 1.8−300 K range. Samples were embedded in solid eicosane to prevent torquing. The ac magnetic susceptibility measurements were performed in an oscillating ac field of 3.5 Oe and a zero dc field. The oscillation frequencies were in the 5−1488 Hz range. Pascal's constants were used to estimate the diamagnetic corrections, which were subtracted from the experimental susceptibilities to give the molar paramagnetic susceptibilities (χ_M).

RESULTS AND DISCUSSION

Syntheses. Many reactions under various conditions and reagent ratios were explored before the procedures described below were developed. These were all variations, to some degree or other, of the comproportionation reaction between Mn^{II} and Mn^{VII} that is the synthetic procedure for $[Mn_{12}O_{12}(O_2CMe)_{16}(H_2O)_4](Mn^{III}{}_8Mn^{IV}{}_4)$.[25] The latter involves the reaction in aqueous acetic acid between $Mn(O_2CMe)_2$ and $KMnO_4$ in a Mn^{II}/Mn^{VII} ratio that gives an average of $Mn^{3.33+}$. We have screened various modifications, such as in the Mn^{II}/Mn^{VII} ratio, the carboxylate identity, and others, and added a Bi^{III} source to target a mixed-metal product.

The reaction between $Mn(O_2CEt)_2\cdot xH_2O$, $N^nBu_4MnO_4$, and $Bi(NO_3)_3\cdot 5H_2O$ in a 10:3:10 molar ratio in 17% aqueous propionic acid led to subsequent isolation of black crystals of $[Bi_2Mn_6O_9(O_2CEt)_9(HO_2CEt)(NO_3)_3]$ (**1**) in small (∼10%) but reproducible yields. An analogous reaction between $Mn(O_2CPh)_2\cdot 2H_2O$, $N^nBu_4MnO_4$, and $Bi(NO_3)_3\cdot 5H_2O$ in the same 10:3:10 ratio but in hot $PhCO_2H$/MeCN (heated to ensure dissolution of all benzoic acid and thus prevent formation of insoluble Mn oxide precipitates) gave the isostructural complex $[Bi_2Mn_6O_9(O_2CPh)_9(HO_2CPh)(NO_3)_3]$ (**2**) in a superior (∼30%) yield. Both **1** and **2** are at the $Bi^{III}{}_2Mn^{IV}{}_6$ oxidation level (vide infra), although the Mn^{II}/Mn^{VII} ratio employed gives an average Mn oxidation state in the solution of only $Mn^{3.15+}$, appreciably lower than the Mn^{4+}. We normally do not expect atmospheric O_2 to generate Mn^{4+} in such reactions, and our feeling is that the Mn^{IV} is likely forming from disproportionation of Mn^{III}; this is consistent with the low yields (10−30% based on total Mn) of isolated products (eq 1). In addition, the filtrates were still intensely colored, but we did not pursue isolation from them of additional crops of **1** or **2**, or other products. Instead, we changed the Mn^{II}/Mn^{VII} ratio to 3:2, which gives an average Mn oxidation state of +4, but these reactions led to even smaller isolated yields of **1** and **2** (∼5−10%), with the main product now being the $[Mn_{12}O_{12}(O_2CR)_{16}(H_2O)_4]$ complexes; the latter cocrystallized in yields as large as 50−60% (based on total available Mn).

$$10Mn^{2+} + 3Mn^{7+} + 2Bi^{3+} \rightarrow Bi_2Mn^{IV}{}_6 + 3Mn^{3+} + 4Mn^{2+} \quad (1)$$

Since **1** and **2** contain bound NO_3^- ions and the latter are thus essential for yielding these products, the $Bi(NO_3)_3\cdot 5H_2O$ reagent was replaced with $Bi(O_2CMe)_3$ to possibly divert the reactions to different types of clusters. Indeed, the comproportionation reaction between $Mn(O_2CPh)_2\cdot 2H_2O$, $N^nBu_4MnO_4$, and $Bi(O_2CMe)_3$ in a 10:3:10 ratio in hot $PhCO_2H/MeNO_2$ led to the subsequent isolation of $[BiMn_{10}O_8(O_2CPh)_{17}(HO_2CPh)(H_2O)]$ (**3**) in good (∼60%) yield. Complex **3** contains $Bi^{III}Mn^{III}{}_{10}$, the Mn^{III} oxidation level now being that expected from the average of +3.15 from the employed Mn^{II}/Mn^{VII} ratio. This rationalizes the much larger isolated yield of **3** compared with **2** and suggests that the presence of the hard nitrate ion facilitates disproportionation and formation of a Mn^{IV}-containing product. An analogous reaction with $Mn(O_2CEt)_2\cdot xH_2O$ and $EtCO_2H$ in place of $Mn(O_2CPh)_2\cdot 2H_2O$ and $PhCO_2H$, respectively, also led to a dark brown solution, but we were unable to isolate any pure products, such as $[BiMn_{10}O_8(O_2CEt)_{17}(HO_2CEt)(H_2O)]$, the propionate analogue of **3**.

dx.doi.org/10.1021/ic200656q |*Inorg. Chem.* 2011, 50, 5272–5282

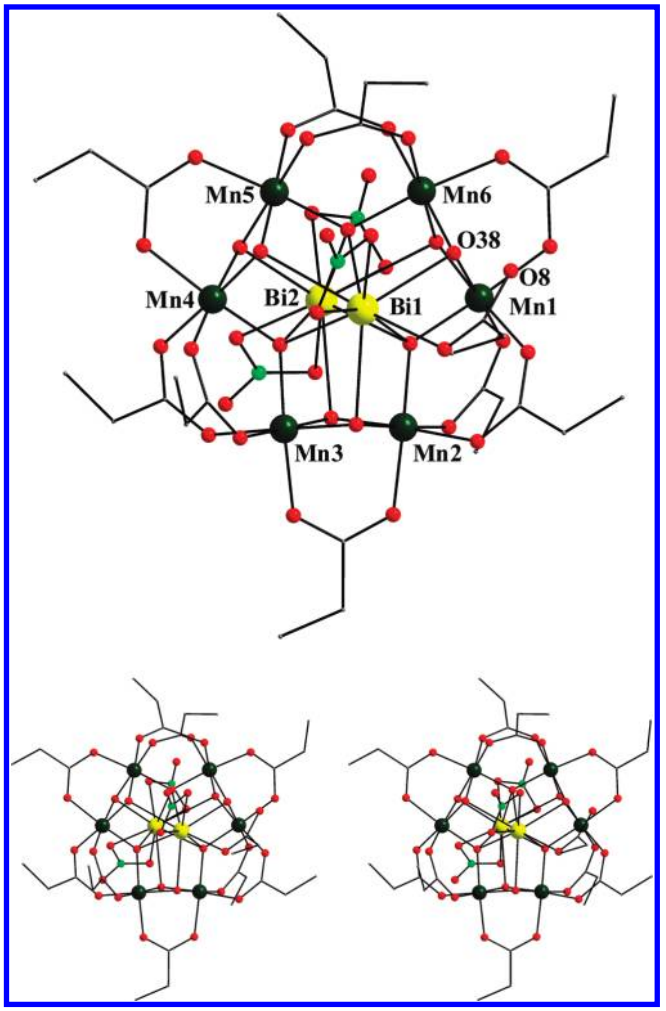

Figure 1. Partially labeled PovRay representation (top) and stereopair (bottom) of complex **1**, with H atoms omitted for clarity. Color scheme: Bi^{III}, yellow; Mn^{IV}, dark green; O, red; N, light green; C, gray.

Description of Structures. A partially labeled representation and a stereoview of complex **1** are shown in Figure 1. Selected interatomic distances are listed in Table 2. Complex **1** crystallizes in monoclinic space group $P2_1/n$ with the $[Bi_2Mn_6O_9(O_2CEt)_9(HO_2CEt)(NO_3)_3]$ molecule lying on a crystallographic inversion center. The core consists of a near-planar Mn^{IV}_6 wheel (displacement of Mn atoms from the Mn_6 least-squares plane is 0.009−0.044 Å), with the edges bridged alternately by $\{(\mu_3\text{-}O)_2(\mu\text{-}O_2CEt)\}$ and $\{(\mu_4\text{-}O)(\mu\text{-}O_2CEt)_2\}$ ligand sets giving Mn···Mn separations of 2.697−2.733 and 3.295−3.303 Å, respectively. The nine oxide ions are also all bound to one or both of the two Bi^{III} ions, Bi1 and Bi2, which lie 1.725 and 1.946 Å, respectively, out of the Mn_6 plane (Figure 2, top). The complex thus contains a $[Bi_2Mn_6(\mu_4\text{-}O)_3(\mu_3\text{-}O)_6]^{12+}$ core (Figure 2, bottom) of virtual D_{3h} symmetry. Ligation at Bi1 is completed by a monodentate $EtCO_2H$ and a bidentate-chelating NO_3^- and at Bi2 by two bidentate-chelating NO_3^- groups. The Mn−O^{2-} (1.807−1.878 Å) and propionate Mn−O (1.924−1.962 Å) bond lengths are typical of Mn^{IV} values,[26] while the Bi^{III}−O bonds are in the range 2.326−2.862 Å, in agreement with values in the literature.[27]

All Mn atoms are six-coordinate with distorted octahedral geometry, whereas Bi1 and Bi2 are nine- and 10-coordinate, respectively.

Table 2. Selected Interatomic Distances (Å) for 1

parameter		parameter	
Mn(1)···Mn(2)	3.303(1)	Bi(1)···Mn(5)	3.468(1)
Mn(2)···Mn(3)	2.697(2)	Bi(1)···Mn(6)	3.427(2)
Mn(3)···Mn(4)	3.295(2)	Bi(2)···Mn(1)	3.721(1)
Mn(4)···Mn(5)	2.733(1)	Bi(2)···Mn(2)	3.610(1)
Mn(5)···Mn(6)	3.295(3)	Bi(2)···Mn(3)	3.562(2)
Mn(6)···Mn(1)	2.717(2)	Bi(2)···Mn(4)	3.445(3)
Bi(1)···Mn(1)	3.416(3)	Bi(2)···Mn(5)	3.478(2)
Bi(1)···Mn(2)	3.492(3)	Bi(2)···Mn(6)	3.708(2)
Bi(1)···Mn(3)	3.522(2)	Bi(1)···Bi(2)	3.677(2)
Bi(1)···Mn(4)	3.497(1)		
Mn(1)−O(1)	1.959(3)	Mn(5)−O(24)	1.853(3)
Mn(1)−O(3)	1.837(3)	Mn(5)−O(31)	1.932(3)
Mn(1)−O(4)	1.934(4)	Mn(5)−O(33)	1.924(4)
Mn(1)−O(36)	1.937(3)	Mn(6)−O(24)	1.853(3)
Mn(1)−O(37)	1.820(3)	Mn(6)−O(32)	1.931(3)
Mn(1)−O(38)	1.869(3)	Mn(6)−O(34)	1.949(4)
Mn(2)−O(2)	1.956(3)	Mn(6)−O(35)	1.939(3)
Mn(2)−O(3)	1.853(3)	Mn(6)−O(37)	1.807(3)
Mn(2)−O(5)	1.962(3)	Mn(6)−O(38)	1.869(3)
Mn(2)−O(6)	1.832(3)	Bi(1)−O(3)	2.409(3)
Mn(2)−O(12)	1.941(3)	Bi(1)−O(6)	2.628(3)
Mn(2)−O(23)	1.833(3)	Bi(1)−O(7)	2.468(3)
Mn(3)−O(6)	1.838(3)	Bi(1)−O(9)	2.416(4)
Mn(3)−O(13)	1.927(3)	Bi(1)−O(10)	2.602(5)
Mn(3)−O(14)	1.956(3)	Bi(1)−O(16)	2.588(3)
Mn(3)−O(17)	1.852(3)	Bi(1)−O(17)	2.482(3)
Mn(3)−O(21)	1.939(3)	Bi(1)−O(24)	2.380(3)
Mn(3)−O(23)	1.826(3)	Bi(1)−O(38)	2.474(3)
Mn(4)−O(15)	1.943(3)	Bi(2)−O(3)	2.651(3)
Mn(4)−O(16)	1.841(3)	Bi(2)−O(17)	2.470(3)
Mn(4)−O(17)	1.840(3)	Bi(2)−O(22)	2.412(3)
Mn(4)−O(18)	1.952(3)	Bi(2)−O(23)	2.656(3)
Mn(4)−O(20)	1.924(3)	Bi(2)−O(24)	2.579(3)
Mn(4)−O(22)	1.878(3)	Bi(2)−O(25)	2.326(3)
Mn(5)−O(16)	1.828(3)	Bi(2)−O(26)	2.692(4)
Mn(5)−O(19)	1.928(4)	Bi(2)−O(28)	2.698(4)
Mn(5)−O(22)	1.872(3)	Bi(2)−O(29)	2.365(4)
		Bi(2)−O(37)	2.862(4)

The metal oxidation states and the protonation levels of O^{2-} ions were suggested by the metric parameters and charge balance considerations and confirmed by bond valence sum (BVS) calculations (Table 3).[28] BVS values for O^{2-} atoms are typically 1.8−2.0, although participation as acceptor atoms in H bonds can decrease this value slightly. In **1**, we note that the μ_4-O^{2-} ions give a slightly greater value of ∼2.2 (which does not affect their assignment as O^{2-}), whereas the μ_3-O^{2-} ions are in the normal range. The monodentate $EtCO_2H$ ligand on Bi1 binds through its C═O group (C7−O7 = 1.251(7) Å), and its COH group (C7−O8 = 1.338 (7) Å) forms a H bond to oxide O38 (O7···O38 = 2.707(5) Å). The H atom (H38) was observed in a difference Fourier map and appeared to lie slightly closer to the oxide O8 (1.279 vs 1.528 Å), but we nevertheless disfavor a suggestion that formally the oxide O38 is really OH^- and the $EtCO_2H$ is $EtCO_2^-$. The O38 BVS (1.79), the binding to Bi through the C═O, and the low basicity (vs $EtCO_2^-$)

dx.doi.org/10.1021/ic200656q |*Inorg. Chem.* 2011, 50, 5272–5282

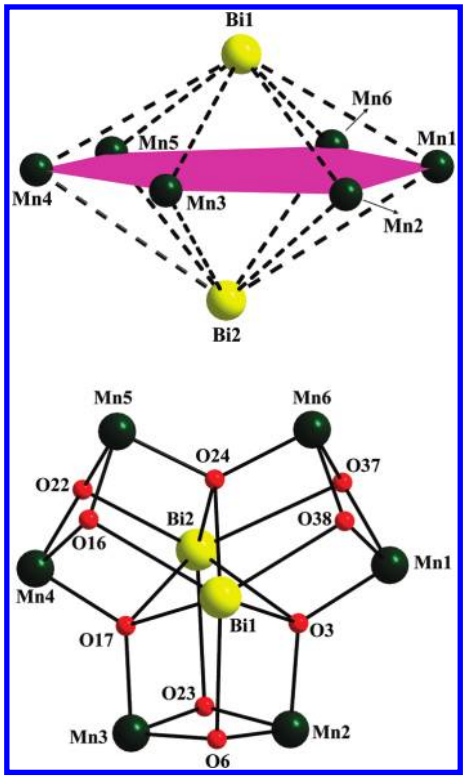

Figure 2. (Top) The Bi_2Mn_6 topology, showing the Mn^{IV}_6 least-squares plane (purple) of the wheel description. The black dashed lines are the Bi···Mn vectors. (Bottom) Labeled PovRay representation of the complete $[Bi_2Mn_6(\mu_4\text{-}O)_3(\mu_3\text{-}O)_6]^{12+}$ core of **1**. Color scheme: Bi^{III}, yellow; Mn^{IV}, dark green; O, red.

Table 3. Bond Valence Sum (BVS)[a,b] Calculations for Mn and Selected O Atoms of 1

atom	Mn^{II}	Mn^{III}	Mn^{IV}
Mn1	4.29	3.92	4.12
Mn2	4.26	3.90	4.09
Mn3	4.33	3.96	4.15
Mn4	4.24	3.88	4.07
Mn5	4.31	3.94	4.14
Mn6	4.31	3.94	4.14

atom	BVS	assignment
O3	2.17	O^{2-} (μ_4)
O6	1.80	O^{2-} (μ_3)
O16	1.83	O^{2-} (μ_3)
O17	2.23	O^{2-} (μ_4)
O22	1.82	O^{2-} (μ_3)
O23	1.81	O^{2-} (μ_3)
O24	2.22	O^{2-} (μ_4)
O37	1.79	O^{2-} (μ_3)
O38	1.78	O^{2-} (μ_3)[c]

[a] The underlined value is the one closest to the charge for which it was calculated. The oxidation state can be taken as the nearest whole number to the underlined value. [b] An O BVS in the ~1.8−2.0, ~1.0−1.2, and ~0.2−0.4 ranges is indicative of non-, single- and double-protonation, respectively, but can be altered somewhat by hydrogen bonding. [c] See the text.

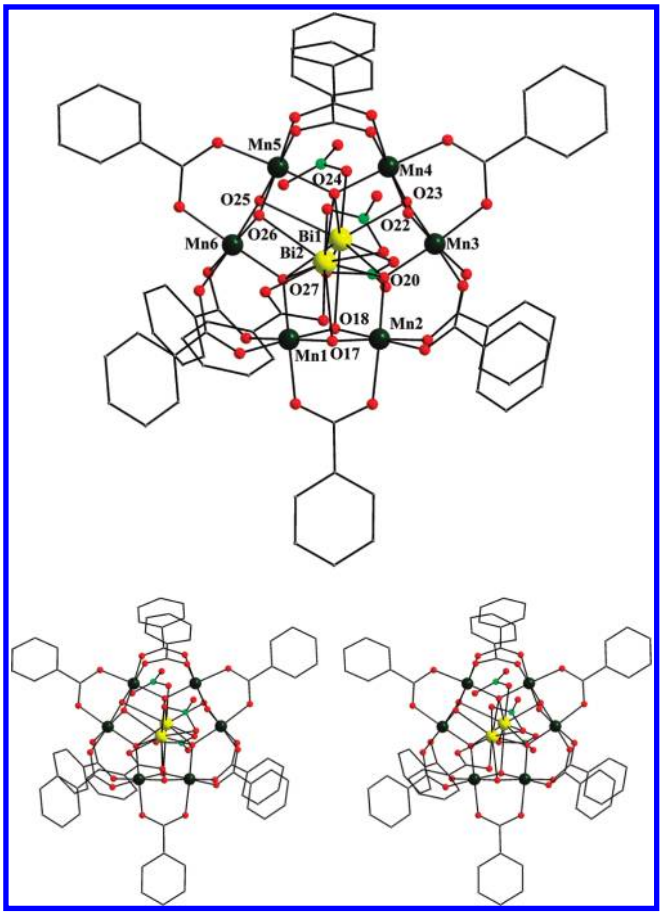

Figure 3. Partially labeled PovRay representation (top) and stereopair (bottom) of complex **2**, with H atoms omitted for clarity. Color scheme: Bi^{III}, yellow; Mn^{IV}, dark green; O, red; N, green; C, gray.

expected for an O^{2-} bridging three high oxidation state metal atoms all suggest O38 is not formally protonated and that the $EtCO_2H$ is protonated. In addition to the above "di-Bi-capped Mn_6 wheel" description of the $[Bi_2Mn_6O_9]^{12+}$ core, an alternative description can be presented: the $[Bi_2Mn_6O_9]$ unit (Figure 2, bottom) can be considered as three $[Bi_2Mn_2(\mu_3\text{-}O)_4]$ distorted cubanes fused together at one of their faces; i.e., each cubane fuses half of one face with one neighbor and the other half of that face with the other neighbor. Finally, there are no significant intermolecular interactions, only weak ones involving C−H bonds.

A partially labeled representation and a stereoview of complex **2** are shown in Figure 3. The molecule is essentially isostructural with complex **1** and thus will not be discussed here. The main differences between **2** and **1** are the benzoate vs propionate identity of the carboxylate employed, which causes a greater separation between neighboring molecules in the crystal, the binding of the $PhCO_2H$ to one Bi as a bidentate chelate rather than monodentate ligand, and the extensive disorder observed in some ligands and the many solvent molecules of crystallization. Again, BVS calculations, charge considerations, and inspection of metric parameters confirm that the Mn and Bi atoms of complex **2** are all in +4 and +3 oxidation states, respectively.

The heterometallic $[M_6M'_2O_9]$ cores of **1** and **2** have never been seen before in the cluster chemistry of any metals. In addition, complexes **1** and **2** are only the second and third examples of a Mn^{IV}_6 wheel. The one previous Mn_6 wheel at this oxidation level

dx.doi.org/10.1021/ic200656q |*Inorg. Chem.* 2011, 50, 5272–5282

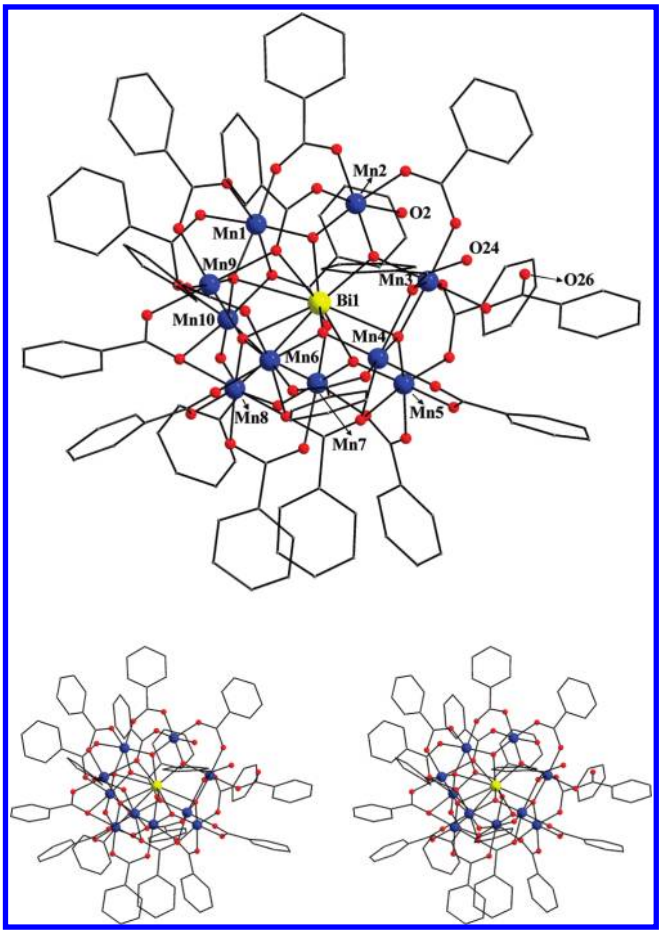

Figure 4. Partially labeled PovRay representation (top) and stereopair (bottom) of complex **3**, with H atoms omitted for clarity. Color scheme: Bi^{III}, yellow; Mn^{III}, blue; O, red; C, gray.

was $[CeMn_6O_9(O_2CMe)_9(NO_3)(H_2O)_2]$, which has a single Ce^{IV} atom at the center and lying 1.513 Å above the Mn_6 plane.[29] In contrast, **1** and **2** are the first examples of a cyclic $M_6M'_2$ unit, i.e., a transition metal M_6 wheel with two central M′ atoms on either side of the wheel plane. They are related to the $CeMn_6$ compound in that they have a second heteroatom on the other side of the Mn_6 plane, which suggests that under the right conditions the analogous compound $[Ce_2Mn_6O_9(O_2CMe)_9(NO_3)_5(H_2O)]$ with Ce^{IV} and/or Ce^{III} might also be attainable. A Cu_6 wheel with a single central lanthanide atom is also known.[30]

A partially labeled representation and a stereoview of complex **3** are shown in Figure 4. Selected interatomic distances are listed in Table 4. Complex **3** crystallizes in the monoclinic space group $P2_1/c$ with the $BiMn_{10}$ molecule in a general position. It contains one Bi^{III} and 10 Mn^{III} atoms held together by four μ_4-O^{2-} (O4, O7, O8, O9) and four μ_3-O^{2-} (O1, O3, O5, O6) ions to give a low symmetry $[BiMn_{10}O_8]^{17+}$ core. There are a variety of familiar smaller nuclearity units that can be seen as fragments of the core, including a $[BiMn_3(\mu_3\text{-}O)_2]^{8+}$ butterfly unit (Bi1, Mn1, Mn2, Mn3, O1, O3), four $[BiMn_3(\mu_4\text{-}O)]^{10+}$ tetrahedra (Bi1, Mn1, Mn9, Mn10, O9/Bi1, Mn3, Mn4, Mn5, O4/Bi1, Mn6, Mn8, Mn9, O7/Bi1, Mn7, Mn8, Mn10, O8), and two $[BiMn_2(\mu_3\text{-}O)]^{7+}$ triangular units (Bi1, Mn4, Mn6, O5/Bi1, Mn5, Mn7, O6), all fused together and linked to adjacent units by sharing common Mn and Bi vertices. As a result, the single nine-coordinate Bi^{III} atom is encapsulated inside a Mn^{III}_{10} cage, held in place by the eight O^{2-} ions and a carboxylate O atom (O17) that bridge it to the Mn atoms (Figure 5). Peripheral ligation about the $[BiMn_{10}O_8]^{17+}$ core is provided by a total of 17 bridging $PhCO_2^-$ groups, one terminal $PhCO_2H$ group, and one H_2O molecule. The $PhCO_2H$ group binds to Mn3 with its O27 and forms a particularly short H bond to the unbound O atom of a neighboring benzoate (O26···O24 = 2.413(10) Å). The terminal H_2O (O2) on Mn2 forms a H bond to the Mn-bound O20 of a neighboring carboxylate (O2···O20 = 2.650(10) Å). The $PhCO_2^-$ groups adopt an impressive variety of bridging modes, and these are shown in Figure 6. Twelve $PhCO_2^-$ groups bridge in the common $\eta^1{:}\eta^1{:}\mu$ mode (**I**), three in the rarer $\eta^1{:}\eta^2{:}\mu_3$ mode (**II**) across Mn3 or BiMn2 units, one in the extremely rare $\eta^2{:}\eta^2{:}\mu_4$ mode (**III**), and the final one in an $\eta^2{:}\mu$ mode (**IV**) leaving O24 unbound. Thus, including the monatomic OR^- bridge (R = $PhCO^-$), **3** contains an overall $[BiMn_{10}(\mu_4\text{-}O)_4(\mu_3\text{-}O)_4(\mu\text{-}OR)_6]^{11+}$ core (Figure 5). The structure does not form any significant intermolecular H

Table 4. Selected Interatomic Distances (Å) for $3\cdot 6PhCO_2H$

parameter		parameter	
Mn···Mn	3.047(3) −6.915(3)	Bi···Mn	3.240(2) −3.758(2)
Mn(1)−O(1)	1.833(7)	Mn(6)−O(38)	1.957(8)
Mn(1)−O(9)	1.955(7)	Mn(7)−O(6)	1.824(7)
Mn(1)−O(10)	1.952(8)	Mn(7)−O(8)	1.912(7)
Mn(1)−O(13)	2.134(9)	Mn(7)−O(14)	2.127(8)
Mn(1)−O(15)	2.363(9)	Mn(7)−O(36)	1.940(8)
Mn(1)−O(46)	1.979(8)	Mn(7)−O(41)	2.239(7)
Mn(2)−O(1)	1.836(7)	Mn(7)−O(43)	1.983(8)
Mn(2)−O(2)	2.301(8)	Mn(8)−O(7)	1.945(8)
Mn(2)−O(3)	1.891(7)	Mn(8)−O(8)	1.919(7)
Mn(2)−O(11)	1.991(8)	Mn(8)−O(34)	2.275(7)
Mn(2)−O(16)	2.122(1)	Mn(8)−O(39)	1.968(8)
Mn(2)−O(18)	1.956(8)	Mn(8)−O(40)	1.924(8)
Mn(3)−O(3)	1.832(7)	Mn(8)−O(44)	2.186(7)
Mn(3)−O(4)	1.910(7)	Mn(9)−O(7)	1.930(7)
Mn(3)−O(19)	1.941(8)	Mn(9)−O(9)	1.908(8)
Mn(3)−O(20)	2.132(8)	Mn(9)−O(12)	1.930(8)
Mn(3)−O(25)	2.343(8)	Mn(9)−O(17)	2.352(9)
Mn(3)−O(27)	1.944(8)	Mn(9)−O(23)	1.965(9)
Mn(4)−O(4)	1.913(7)	Mn(9)−O(45)	2.198(9)
Mn(4)−O(5)	1.853(8)	Mn(10)−O(8)	1.897(7)
Mn(4)−O(25)	2.380(8)	Mn(10)−O(9)	1.916(7)
Mn(4)−O(29)	1.942(8)	Mn(10)−O(15)	2.167(8)
Mn(4)−O(31)	1.947(8)	Mn(10)−O(42)	1.952(8)
Mn(4)−O(35)	2.226(8)	Mn(10)−O(44)	2.191(8)
Mn(5)−O(4)	1.886(7)	Mn(10)−O(47)	1.974(8)
Mn(5)−O(6)	1.830(7)	Bi(1)−O(1)	2.377(6)
Mn(5)−O(21)	2.117(8)	Bi(1)−O(3)	2.190(7)
Mn(5)−O(28)	1.986(8)	Bi(1)−O(4)	2.678(7)
Mn(5)−O(35)	2.492(7)	Bi(1)−O(5)	2.350(7)
Mn(5)−O(37)	1.966(8)	Bi(1)−O(6)	2.415(8)
Mn(6)−O(5)	1.848(8)	Bi(1)−O(7)	2.716(7)
Mn(6)−O(7)	1.920(7)	Bi(1)−O(8)	2.826(8)
Mn(6)−O(22)	2.097(1)	Bi(1)−O(9)	2.894(7)
Mn(6)−O(30)	1.928(8)	Bi(1)−O(17)	2.491(9)
Mn(6)−O(34)	2.225(8)		

dx.doi.org/10.1021/ic200656q |*Inorg. Chem.* 2011, 50, 5272–5282

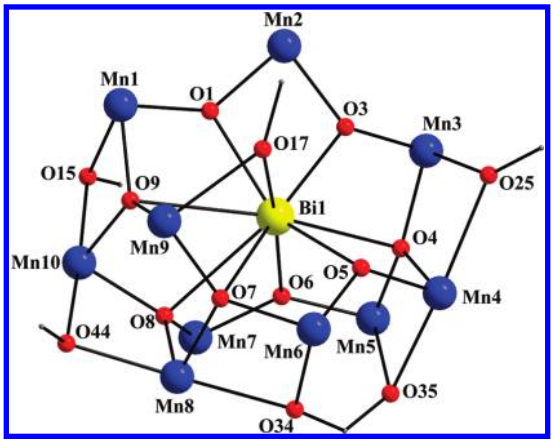

Figure 5. Labeled PovRay representation of the complete $[BiMn_{10}(\mu_4\text{-}O)_4(\mu_3\text{-}O)_4(\mu\text{-}OR)_6]^{11+}$ unit. Color scheme: Bi^{III}, yellow; Mn^{III}, blue; O, red; C, gray.

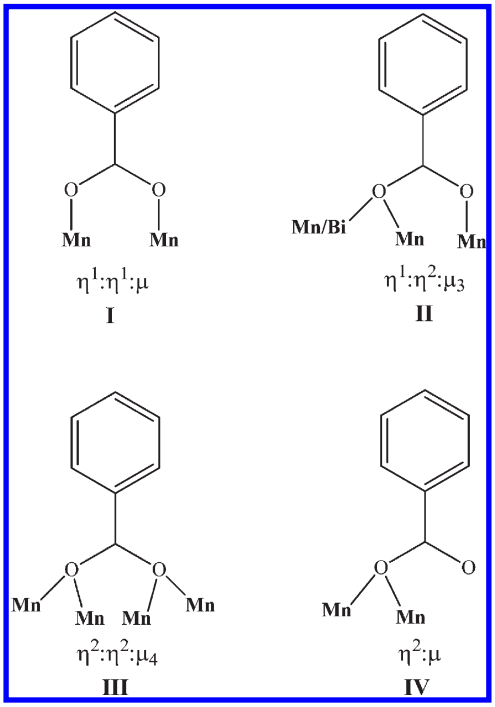

Figure 6. The bridging modes displayed by the $PhCO_2^-$ groups in complex **3**.

bonds, only weak contacts between C−H bonds and the π system of $PhCO_2^-$ groups. Finally, a space-filling representation (Figure 7) shows that **3** has an aesthetically pleasing, near-spherical structure of ∼20 Å diameter.

The Mn atoms are all six-coordinate with near-octahedral geometry. The metal oxidation states and the protonation levels of O^{2-} and H_2O groups were determined by BVS calculations (Table 5),[28] inspection of metric parameters, charge balance considerations, and clear observation of Jahn−Teller (JT) distortion axes at all of the Mn ions. The JT distortions all take the form of axial elongations, as is almost always the case for high-spin Mn^{III}, with JT elongated bonds being 0.1−0.4 Å longer than the other Mn^{III}−O bonds (∼1.8−2.0 Å). Further, the axial positions of the MnO_6 distorted octahedra are all occupied by the

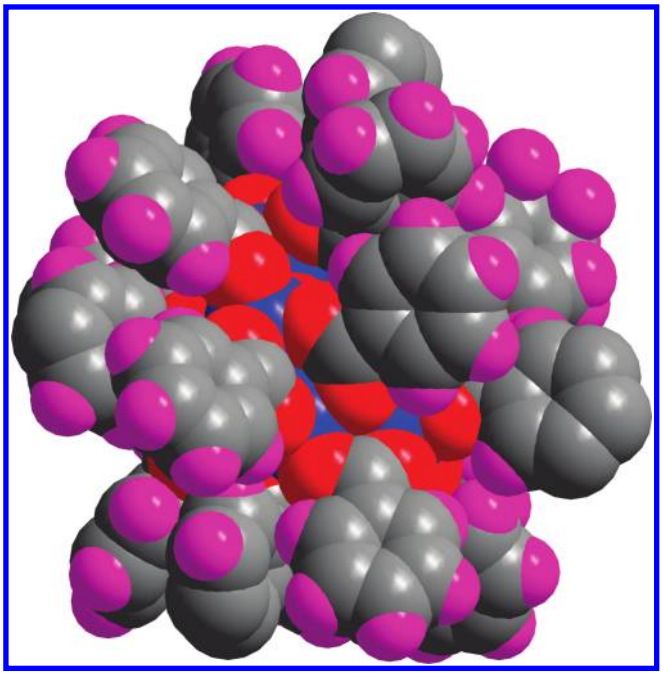

Figure 7. A space-filling representation of **3**. Color scheme: Bi^{III}, yellow; Mn^{III}, blue; O, red; C, gray; H, purple.

Table 5. Bond Valence Sum (BVS)[a,b] Calculations for Mn and Selected Oxygen Atoms in 3

atom	Mn^{II}	Mn^{III}	Mn^{IV}
Mn1	3.16	2.89	3.04
Mn2	3.29	3.01	3.16
Mn3	3.33	3.04	3.20
Mn4	3.17	2.90	3.04
Mn5	3.22	2.94	3.09
Mn6	3.39	3.10	3.26
Mn7	3.36	3.07	3.22
Mn8	3.08	2.81	2.95
Mn9	3.06	2.80	2.94
Mn10	3.19	2.92	3.06

	BVS	assignment
O1	1.92	O^{2-} (μ_3)
O3	2.12	O^{2-} (μ_3)
O4	1.99	O^{2-} (μ_4)
O5	1.89	O^{2-} (μ_3)
O6	1.91	O^{2-} (μ_3)
O7	1.83	O^{2-} (μ_4)
O8	1.89	O^{2-} (μ_4)
O9	1.79	O^{2-} (μ_4)
O2	0.21	H_2O (η^1)

[a] See footnote a of Table 3. [b] See footnote b of Table 3.

O atoms of the carboxylate and water groups. Thus, as is almost always the case, the JT elongation axes avoid the Mn^{III}−O^{2-} bonds, the shortest and strongest in the molecule.[31] The 10 JT elongation axes do not align parallelly but instead in a somewhat random manner (Figure S1, Supporting Information), suggesting the axial zero-field parameter (D) for **3** is very likely to be very

dx.doi.org/10.1021/ic200656q |*Inorg. Chem.* 2011, 50, 5272–5282

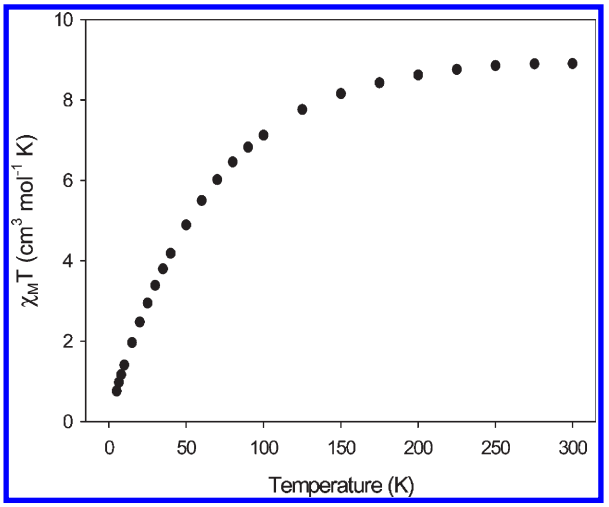

Figure 8. $\chi_M T$ vs T plot for complex **2** in a 1 kG dc field.

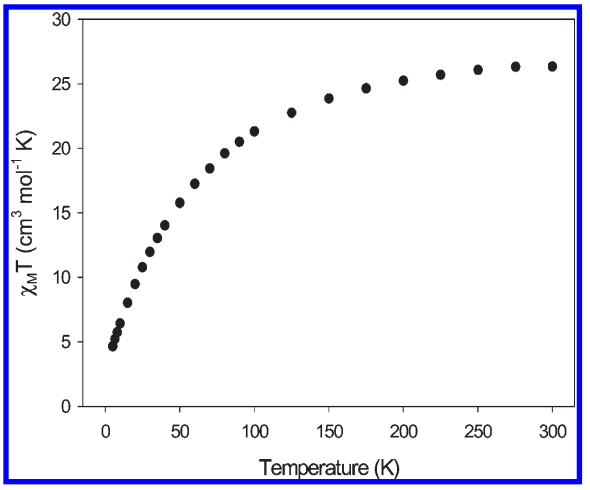

Figure 9. $\chi_M T$ vs T plot for complex **3**·6PhCO$_2$H in a 1 kG dc field.

small (<0.1 cm^{-1}). Complex **3** joins a handful of structurally characterized, heterometallic undecanuclear metal complexes,[32] and it is the first with such a metal core topology and a 10:1 metal composition. Further, the Mn^{III}_{10} shell within the structure of **3** becomes a new member of the small family of decanuclear Mn clusters at the 3+ oxidation state level.[25b,33]

Magnetic Susceptibility Studies on Complexes 1−3. Variable-temperature, solid-state magnetic susceptibility measurements were performed on powdered polycrystalline samples of dried **1**, **2**, and **3**·6PhCO$_2$H restrained in eicosane to prevent torquing, in a 1 kOe (0.1 T) field and in the 5.0−300 K range. All paramagnetism is associated with the Mn ions because Bi^{III} is diamagnetic.

The magnetic data for **1** and **2** are essentially identical, and therefore only those of the latter will be discussed in detail. The data for **1** are available in the Supporting Information. The obtained data for **2** are shown as $\chi_M T$ versus T in Figure 8. $\chi_M T$ steadily decreases from 8.91 cm^3 K mol^{-1} at 300 K to 0.76 cm^3 K mol^{-1} at 5.0 K, which indicates the presence of dominant antiferromagnetic exchange interactions within the molecule. The calculated spin-only (g = 2.0) $\chi_M T$ for a Mn^{IV}_6 cluster of noninteracting metal ions is 11.25 cm^3 K mol^{-1}, appreciably higher than the experimental value at 300 K and thus suggestive of strong antiferromagnetic interactions, as indeed expected for oxide-bridged Mn^{IV}_2 interactions. The $\chi_M T$ value at 5.0 K strongly indicates an S = 0 ground state spin value for **2**, which is as found previously for [CeMn$_6$O$_9$(O$_2$CMe)$_9$(NO$_3$)(H$_2$O)$_2$]. The exchange interactions in the Mn^{IV}_6 wheel of the latter compound have already been studied in extensive detail, having been determined experimentally by fitting the magnetic susceptibility data by matrix diagonalization, and theoretically by ZILSH calculations.[29] The obtained values were found to be weakly antiferromagnetic, $J_1 = -5.8(3)$ cm^{-1} and $J_2 = -0.63(10)$ cm^{-1} ($\mathscr{H} = -2J\hat{S}_i \cdot \hat{S}_j$ convention), where J_1 and J_2 are the interactions for the {Mn$_2$O$_2$(O$_2$CR)} and {Mn$_2$O(O$_2$CR)$_2$} bridged pairs. Given the analogous S = 0 ground states of **1** and **2**, and the fact that we did not anticipate that their interactions would be particularly different from the CeMn$_6$ compound, we did not consider it worthwhile to also carry out a fitting of their data by matrix diagonalization. The topology of the Mn$_6$ wheel also does not allow application of the more convenient Kambe method.[34]

For **3**·6PhCO$_2$H, the obtained data are shown as $\chi_M T$ versus T in Figure 9. $\chi_M T$ steadily decreases from 26.35 cm^3 K mol^{-1} at 300 K to 4.66 cm^3 K mol^{-1} at 5.0 K. Again, the 300 K value is much less than the spin-only (g = 2) value of 30 cm^3 K mol^{-1} for 10 noninteracting Mn^{III} ions, indicating the presence of dominant antiferromagnetic exchange interactions and a low, but likely nonzero, ground state S. The high nuclearity and low symmetry of the complex preclude determination of the individual pairwise Mn_2 exchange interaction parameters, and we concentrated instead on characterizing the ground state spin S by fits of low temperature magnetization data. Magnetization (M) data were collected in the 1−70 kG magnetic field and 1.8−10.0 K temperature ranges. However, we could not get an acceptable fit using data collected over the whole field range, which is a common problem caused by low-lying excited states in high nuclearity complexes, especially if some have an S value greater than that of the ground state, as is the case for **3**·6PhCO$_2$H on the basis of Figure 9. A common solution is to only use data collected with low fields (≤1.0 T), as previously reported for high-nuclearity Mn^{III} clusters,[35] but in this case, it was still not possible to obtain a satisfactory fit assuming that only the ground state is populated. This suggests particularly low-lying excited states in this compound. Thus, we turned to ac susceptibility measurements as an alternative means of determining the ground state.

As we have described before on multiple occasions,[35] ac susceptibility studies are a powerful complement to dc methods for determining ground states because they preclude any complications arising from low-lying excited states and/or the presence of a dc field. These were performed in the 1.8−15 K range using a 3.5 G ac field oscillating at frequencies in the 50−1000 Hz range. If the magnetization vector stays in phase with the oscillating field, there is no out-of-phase susceptibility (χ''_M) signal, and the in-phase susceptibility (χ'_M) is equal to the dc susceptibility. Figure 10 shows the in-phase ac susceptibility for **3**·6PhCO$_2$H, plotted as $\chi'_M T$ versus T, together with the plot for **2** for comparison. For **2**, $\chi'_M T$ decreases only slightly in this temperature range, from ∼0.5 to ∼0.1 cm^3 K mol^{-1}, and is clearly heading for ∼0 cm^3 K mol^{-1}, confirming an S = 0 ground state that is well isolated from excited states; i.e., there is little population of the latter up to 15 K. In contrast, $\chi'_M T$ for **3**·6PhCO$_2$H decreases steeply from ∼7.5 cm^3 K mol^{-1} at 15 K to under 3 cm^3 K mol^{-1} at 1.8 K, indicating extensive of depopulation of low-lying excited states with S greater than the ground state and confirming the latter as the reason for the poor magnetization fits. Extrapolation of the $\chi'_M T$

dx.doi.org/10.1021/ic200656q |*Inorg. Chem.* 2011, 50, 5272–5282

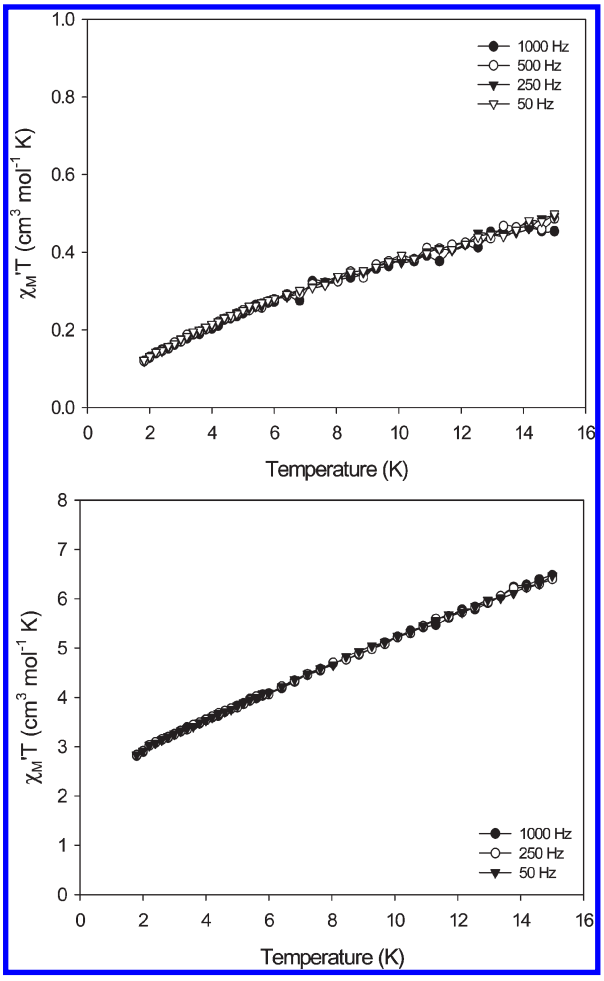

Figure 10. In-phase ac susceptibility (χ'_M) as $\chi'_M T$ vs T for **2** (top) and **3**·6PhCO$_2$H (bottom) at the indicated frequencies.

plot from above 2 to 0 K gives a value of ~2.6 cm^3 K mol^{-1}, which is consistent with an $S = 2$ ground state and $g < 2$, as expected for a Mn^{III} cluster; the spin-only ($g = 2.0$) $\chi'_M T$ for $S = 1$, 2, and 3 states is 1.0, 3.0, and 6.0 cm^3 K mol^{-1}, respectively. Thus, complex **3**·6PhCO$_2$H has a small ground state spin and, in combination with only the small anisotropy suggested by the orientation of the 10 Mn^{III} JT axes, should not result in any significant barrier to magnetization relaxation. This is confirmed by the absence of out-of-phase ac susceptibility signals down to 1.8 K (Figure S4).

CONCLUSIONS

The described work has led to the discovery of the first polynuclear Bi/Mn complexes at high (Mn$^{III/IV}$) oxidation states. On the basis of the two structural types obtained to date, at least, the incorporation of Bi^{III} into Mn carboxylate cluster chemistry leads to products that are not structurally congruent with any currently known Mn or Mn/Ln (Ln = lanthanide) carboxylate cluster. The Bi$_2$Mn$_6$ and BiMn$_{10}$ topologies are structurally very interesting, although they do not correspond to fragments of the structure of a mixed Bi/Mn oxide. Further, in spite of these first Bi/Mn molecular clusters not having particularly exciting magnetic properties, i.e., they are not new SMMs, they do not have particularly high ground state spin values, etc.; the described work does indicate that the use of Bi^{III} provides access to structurally interesting heterometallic Bi/Mn clusters and suggests that further studies are warranted as a potential route to new structural types. Indeed, the work described represents merely our first steps in a full development of oxide-bridged Bi/Mn molecular cluster chemistry, and results to date augur well for possible access to molecular analogs of the multifunctional Bi/Mn/O solids that are of such great interest in materials science.

ASSOCIATED CONTENT

Supporting Information. Structural and magnetism figures and X-ray crystallographic files in CIF format for complexes **1**, **2**·4MeCN·2CH$_2$Cl$_2$, and **3**·6PhCO$_2$H. This material is available free of charge via the Internet at http://pubs.acs.org.

AUTHOR INFORMATION

Corresponding Author
*E-mail: christou@chem.ufl.edu.

ACKNOWLEDGMENT

This work was supported by NSF Grant CHE-0910472.

REFERENCES

(1) (a) Ferreira, K. N.; Iverson, T. M.; Maghlaoui, K.; Barber, J; Iwata, S. *Science* **2004**, *303*, 1831. (b) Carrell, T. G.; Tyryshkin, A. M.; Dismukes, G. C. *J. Biol. Inorg. Chem.* **2002**, *7*, 2. (c) Cinco, R. M.; Rompel, A.; Visser, H.; Aromi, G.; Christou, G.; Sauer, K.; Klein, M. P.; Yachandra, V. K. *Inorg. Chem.* **1999**, *38*, 5988. (d) Yachandra, V. K.; Sauer, K.; Klein, M. P. *Chem. Rev.* **1996**, *96*, 2927.(e) *Manganese Compounds as Oxidizing Agents in Organic Chemistry*; Arndt, D.; Ed.; Open Court Publishing Company: Chicago, IL, 1981. (f) Snider, B. B. *Chem. Rev.* **1996**, *96*, 339.(g) Ho, T.-L. *Organic Syntheses By Oxidation With Metal Compounds*; Mijs, W. J., de Jonge, C. R. H. I., Eds.; Plenum Press: New York, 1986; Chapter 11, pp 569−631. (h) Trovarelli, A. *Catal. Rev.* **1996**, *38*, 439. (i) Mehring, M. *Coord. Chem. Rev.* **2007**, *251*, 974. (j) Limberg, C. *Angew. Chem., Int. Ed.* **2003**, *42*, 5932. (k) Gaspard-Iloughmane, H.; Le Roux, C. *Eur. J. Org. Chem.* **2004**, 2517.

(2) (a) Law, N. A.; Caudle, M. T.; Pecoraro, V. L. In *Advances in Inorganic Chemistry*; Sykes, A. G.; Ed.; Academic Press: London, 1998; Vol. 46, p 305. (b) Cinco, R. M.; Holman, K. L. M.; Robblee, J. H.; Yano, J.; Pizarro, E.; Bellacchio, E.; Sauer, K.; Yachandra, V. K. *Biochemistry* **2002**, *41*, 12928. (c) Loll, B.; Kern, J.; Saenger, W.; Zouni, A.; Biesiadka, J. *Nature* **2005**, *438*, 1040. (d) Yano, J.; Kern, J.; Sauer, K.; Latimer, M. J.; Pushkar, Y.; Biesiadka, J.; Loll, B.; Saenger, W.; Messinger, J.; Zouni, A.; Yachandra, V. K. *Science* **2006**, *314*, 821 and references therein.

(3) (a) Nugent, J. *Biochim. Biophys. Acta: Bioenerg.* **2001**, *1503*, 1–259. (b) Ruttinger, W.; Dismukes, C. G. *Chem. Rev.* **2001**, *101*, 21. (c) Mukhopadhyay, S.; Mandal, S. K.; Bhaduri, S.; Armstrong, W. H. *Chem. Rev.* **2004**, *104*, 3981–4026. (d) Hewitt, I. J.; Tang, J.-K.; Madhu, N. T.; Clerac, R.; Buth, G.; Anson, C. E.; Powell, A. K. *Chem. Commun.* **2006**, 2650.

(4) (a) Sun, H. Z.; Szeto, K. Y. *J. Inorg. Biochem.* **2003**, *94*, 114. (b) Hutson, J. C. *J. Appl. Toxicol.* **2005**, *25*, 234. (c) Islek, I.; Uysal, S.; Gok, F.; Dundaroz, R.; Kucukoduk, S. *Pediatr. Nephrol.* **2001**, *16*, 510.

(5) (a) Mehring, M.; Mansfeld, D.; Paalasmaa, S.; Schürmann, M. *Chem.—Eur. J.* **2006**, *12*, 1767. (b) Mehring, M.; Paalasmaa, S.; Schürmann, M. *Eur. J. Inorg. Chem.* **2005**, 4891.

(6) (a) Stamatatos, Th. C.; Abboud, K. A.; Wernsdorfer, W.; Christou, G. *Angew. Chem., Int. Ed.* **2007**, *46*, 884. (b) Wang, W.-G.; Zhou, A.-J.; Zhang, W.-X.; Tong, M.-L.; Chen, X.-M; Nakano, M.; Beedle, C. C.; Hendrickson, D. N. *J. Am. Chem. Soc.* **2007**, *129*, 1014. (c) Murugesu, M.; Habrych, M.; Wernsdorfer, W.; Abboud, K. A.;

Christou, G. *J. Am. Chem. Soc.* **2004**, *126*, 4766. (d) Murugesu, M.; Takahashi, S.; Wilson, A.; Abboud, K. A.; Wernsdorfer, W.; Hill, S.; Christou, G. *Inorg. Chem.* **2008**, *47*, 9459. (e) Ako, A. M.; Hewitt, I. J.; Mereacre, V.; Clérac, R.; Wernsdorfer, W.; Anson, C. E.; Powell, A. K. *Angew. Chem., Int. Ed.* **2006**, *45*, 4926. (f) Waldmann, O.; Ako, A. M.; Güdel, H. U.; Powell, A. K. *Inorg. Chem.* **2008**, *47*, 3486. (g) Moushi, E. E.; Stamatatos, Th. C.; Wernsdorfer, W.; Nastopoulos, V.; Christou, G.; Tasiopoulos, A. J. *Inorg. Chem.* **2009**, *48*, 5049. (h) Nayak, S.; Beltran, L. M. C.; Lan, Y.; Clérac, R.; Hearns, N. G. R.; Wernsdorfer, W.; Anson, C. E.; Powell, A. K. *Dalton Trans.* **2009**, 1901. (i) Stamatatos, Th. C.; Abboud, K. A.; Wernsdorfer, W.; Christou, G. *Angew. Chem., Int. Ed.* **2006**, *45*, 4134. (j) Stamatatos, Th. C.; Poole, K. M.; Abboud, K. A.; Wernsdorfer, W.; O'Brien, T. A.; Christou, G. *Inorg. Chem.* **2008**, *47*, 5006. (k) Manoli, M.; Johnstone, R. D. L.; Parsons, S.; Murrie, M.; Affronte, M.; Evangelisti, M.; Brechin, E. K. *Angew. Chem., Int. Ed.* **2007**, *46*, 4456.

(7) For some representative references, see: (a) Christou, G.; Gatteschi, D.; Hendrickson, D. N.; Sessoli, R. *MRS Bull.* **2000**, *25*, 66. (b) Sessoli, R.; Tsai, H.-L.; Schake, A. R.; Wang, S.; Vincent, J. B.; Folting, K.; Gatteschi, D.; Christou, G.; Hendrickson, D. N. *J. Am. Chem. Soc.* **1993**, *115*, 1804.

(8) (a) Bircher, R.; Chaboussant, G.; Dobe, D.; Güdel, H. U.; Oshsenbein, S. T.; Sieber, A.; Waldmann, O *Adv. Funct. Mater.* **2006**, *16*, 209. (b) Gatteschi, D.; Sessoli, R. *Angew. Chem., Int. Ed.* **2003**, *42*, 268. (c) Aubin, S. M. J.; Gilley, N. R.; Pardi, L.; Krzystek, J.; Wemple, M. W.; Brunel, L.-C.; Maple, M. B.; Christou, G.; Hendrickson, D. N. *J. Am. Chem. Soc.* **1998**, *120*, 4991. (d) Oshio, H.; Nakano, M. *Chem.—Eur. J.* **2005**, *11*, 5178.

(9) (a) Friedman, J. R.; Sarachik, M. P. *Phys. Rev. Lett.* **1996**, *76*, 3830. (b) Thomas, L.; Lionti, L.; Ballou, R.; Gatteschi, D.; Sessoli, R.; Barbara, B. *Nature* **1996**, *383*, 145.

(10) (a) Wernsdorfer, W.; Sessoli, R. *Science* **2000**, 2417. (b) Wernsdorfer, W.; Soler, M.; Christou, G.; Hendrickson, D. N. *J. Appl. Phys.* **2002**, *91*, 7164. (c) Wernsdorfer, W.; Chakov, N. E.; Christou, G. *Phys. Rev. Lett.* **2005**, *95*, 037203–4.

(11) Bogani, L.; Wernsdorfer, W. *Nat. Mater* **2008**, *7*, 179.

(12) Leuenberger, M. N.; Loss, D. *Nature* **2001**, *410*, 789.

(13) (a) Cabot, A.; Marsal, A.; Arbiol, J.; Morante, J. R. *Sens. Actuatators, B* **2004**, *99*, 74. (b) Shuk, P.; Wiemhöfer, H. D.; Guth, U.; Göpel, W.; Greenblatt, M. *Solid State Ionics* **1996**, *89*, 179.

(14) (a) Yoneda, Y.; Mizuki, J.; Katayama, R.; Yagi, K.; Terauchi, H.; Hamazaki, S.; Takashige, M. *Appl. Phys. Lett.* **2003**, *83*, 275. (b) Liu, W. L.; Xia, H. R.; Han, H.; Wang, X. Q. *J. Mater. Sci.* **2005**, *40*, 1827. (c) Liu, J. B.; Wang, H.; Hou, Y. D.; Zhu, M. K.; Yan, H.; Yoshimura, M. *Nanotechnology* **2004**, *15*, 777. (d) Kudo, A.; Omori, K.; Kato, H. *J. Am. Chem. Soc.* **1999**, *121*, 11459. (e) Cava, R. J.; Batlogg, B.; Krajewski, J. J.; Farrow, R.; Rupp, L. W., Jr.; White, A. E.; Short, K.; Peck, W. F.; Kometami, T. *Nature* **1988**, *332*, 814.

(15) (a) Khomskii, D. I. *J. Magn. Magn. Mater.* **2006**, *306*, 1. (b) Baettig, P.; Seshadri, R.; Spaldin, N. A. *J. Am. Chem. Soc.* **2007**, *129*, 9854. (c) Tokura, Y. *Science* **2006**, *312*, 1481. (d) Cheong, S.-W.; Mostovoy, M. *Nat. Mater.* **2007**, *6*, 13.

(16) (a) Hill, N. A.; Seshadri, R. *Chem. Mater.* **2001**, *13*, 2892. (b) Hill, N. A.; Rabe, K. M. *Phys. Rev. B* **1999**, *59*, 8759. (c) Yamazaki, Y.; Miyasaka, S.; Kaneko, Y.; He, J.-P.; Arima, T.; Tokura, Y. *Phys. Rev. Lett.* **2006**, *96*, 207204. (d) Schmid, H. *Ferroelectrics* **1994**, *162*, 317. (e) Chi, Z. H.; Yang, H.; Feng, S. M.; Li, F. Y.; Yu, R. C.; Jin, C. Q. *J. Magn. Magn. Mater.* **2007**, *310*, e358.

(17) Dikarev, E. V.; Zhang, H.; Li, B. *J. Am. Chem. Soc.* **2005**, *127*, 6156.

(18) (a) Zaleski, C. M.; Depperman, E. C.; Kampf, J. W.; Kirk, M.-L.; Pecoraro, V. L. *Angew. Chem., Int. Ed.* **2004**, *43*, 3912. (b) Mishra, A.; Wernsdorfer, W.; Abboud, K. A.; Christou, G. *J. Am. Chem. Soc.* **2004**, *126*, 15648. (c) Mishra, A.; Wernsdorfer, W.; Parsons, S.; Christou, G.; Brechin, E. K. *Chem. Commun.* **2005**, 2086. (d) Mereacre, V.; Ako, A. M.; Clerac, R.; Wernsdorfer, W.; Filoti, G.; Bartolome, J.; Anson, C. E.; Powell, A. K. *J. Am. Chem. Soc.* **2007**, *129*, 9248. (e) Mereacre, V.; Ako, A. M.; Clerac, R.; Wernsdorfer, W.; Hewitt, I. J.; Anson, C. E.; Powell, A. K. *Chem.—Eur. J.* **2008**, *14*, 3577. (f) Stamatatos, T. C.; Teat, S. J.; Wernsdorfer, W.; Christou, G. *Angew. Chem., Int. Ed.* **2009**, *48*, 521. (g) Karotsis, G.; Kennedy, S.; Teat, S. J.; Beavers, C. M.; Fowler, D. A.; Morales, J. J.; Evangelisti, M.; Dalgarno, S. J.; Brechin, E. K. *J. Am. Chem. Soc.* **2009**, *132*, 12983. (h) Langley, S.; Moubaraki, B.; Murray, K. S. *Dalton Trans.* **2010**, *39*, 5066. (i) Mereacre, V.; Lan, Y.; Clerac, R.; Ako, A. M.; Hewitt, I. J.; Wernsdorfer, W.; Buth, G.; Anson, C. E.; Powell, A. K. *Inorg. Chem.* **2010**, *49*, 5293. (j) Liu, C.-M.; Zhang, D.-Q.; Zhu, D.-B. *Dalton Trans.* **2010**, *39*, 11325.

(19) For example, see: (a) Tasiopoulos, A. J.; Vinslava, A.; Wernsdorfer, W.; Abboud, K. A.; Christou, G. *Angew. Chem., Int. Ed.* **2004**, *43*, 2117. (b) Soler, M.; Wernsdorfer, W.; Folting, K.; Pink, M.; Christou, G. *J. Am. Chem. Soc.* **2004**, *126*, 2156. (c) Dikarev, E. V.; Zhang, H.; Li, B. *Angew. Chem., Int. Ed.* **2006**, *45*, 5448.

(20) Aromi, G.; Bhaduri, S.; Artús, P.; Huffman, J. C.; Hendrickson, D. N.; Christou, G. *Polyhedron* **2002**, *21*, 1779.

(21) Wemple, M. W.; Tsai, H.-L.; Wang, S.; Claude, J. P.; Streib, W. E.; Huffman, J. C.; Hendrickson, D. N.; Christou, G. *Inorg. Chem.* **1996**, *35*, 6437.

(22) Vincent, J. B.; Chang, H.-R.; Folting, K.; Huffman, J. C.; Christou, G.; Hendrickson, D. N. *J. Am. Chem. Soc.* **1987**, *109*, 5703 and references therein.

(23) *SHELXTL6*; Bruker-AXS: Madison, WI, 2000.

(24) Van der Sluis, P.; Spek, A. L. *Acta Crystallogr., Sect. A* **1990**, *A46*, 194.

(25) (a) Bagai, R.; Christou, G. *Chem. Soc. Rev.* **2009**, *38*, 1011. (b) Harden, N. C.; Bolcar, M. A.; Wernsdorfer, W.; Abboud, K. A.; Streib, W. E.; Christou, G. *Inorg. Chem.* **2003**, *42*, 7067. (c) Stamatatos, Th. C.; Vinslava, A.; Abboud, K. A.; Christou, G. *Chem. Commun.* **2009**, 2839.

(26) For example, see: (a) Bhaduri, S.; Pink, M.; Christou, G. *Chem. Commun.* **2002**, 2352. (b) Bhaduri, S.; Tasiopoulos, A. J.; Bolcar, M. A.; Abboud, K. A.; Streib, W. E.; Christou, G. *Inorg. Chem.* **2003**, *42*, 1483. (c) Tasiopoulos, A. J.; Abboud, K. A.; Christou, G. *Chem. Commun.* **2003**, 580.

(27) For example, see: (a) Whitmire, K. H.; Hoppe, S.; Sydora, O.; Jolas, J. L.; Jones, C. M. *Inorg. Chem.* **2000**, *39*, 85. (b) Pell, J. W.; Davis, W. C.; zur Loye, H. C. *Inorg. Chem.* **1996**, *35*, 5754. (c) Thurston, J. H.; Whitmire, K. H. *Inorg. Chem.* **2003**, *42*, 2014.

(28) BVS values are 3.13 for Bi1 and 3.03 for Bi2 in **1** and 3.15 for Bi1 in **3**. We employed a B_0 value of 0.37 Å, and r_0 = 2.094 Å for a Bi^{III}—O bond. (a) Brown, I. D.; Altermatt, D. *Acta Crystallogr., Sect. B* **1985**, *41*, 244. (b) Liu, W.; Thorp, H. H. *Inorg. Chem.* **1993**, *32*, 4102.

(29) Tasiopoulos, A. J.; Milligan, P. L., Jr.; Abboud, K. A.; O'Brien, T. A.; Christou, G. *Inorg. Chem.* **2007**, *46*, 9678.

(30) Zhang, Y.-J.; Ma, B.-Q.; Gao, S.; Li, J.-R.; Liu, Q.-D.; Wen, G.-H.; Zhang, X.-X. *Dalton Trans.* **2000**, 2249.

(31) For example, see: Chakov, N. E.; Lee, S.-C.; Harter, A. G.; Kuhns, P. L.; Reyes, A. P.; Hill, S. O.; Dalal, N. S.; Wernsdorfer, W.; Abboud, K. A.; Christou, G. *J. Am. Chem. Soc.* **2006**, *128*, 6975.

(32) (a) Tsai, H.-L.; Wang, S.; Folting, K.; Streib, W. E.; Hendrickson, D. N.; Christou, G. *J. Am. Chem. Soc.* **1995**, *117*, 2503. (b) Shiga, T.; Onuki, T.; Matsumoto, T.; Nojiri, H.; Newton, G. N.; Hoshino, N.; Oshio, H. *Chem. Commun.* **2009**, 3568. (c) Kessler, V. G.; Panov, A. N.; Borissevitch, A. Y.; Turova, N. Y. *J. Sol.-Gel. Sci. Technol.* **1998**, *12*, 81. (d) Berlinguette, C. P.; Dunbar, K. R. *Chem. Commun.* **2005**, 2451.

(33) (a) John, R. P.; Lee, K.; Kim, B. J.; Suh, B. J.; Rhee, H.; Lah, M. S. *Inorg. Chem.* **2005**, *44*, 7109. (b) Liu, S.-X.; Lin, S.; Lin, B.-Z.; Lin, C.-C.; Huang, J.-Q. *Angew. Chem., Int. Ed.* **2001**, *40*, 1084. (c) Eppley, H. J.; Aubin, S. M. J.; Streib, W. E.; Bollinger, J. C.; Hendrickson, D. N.; Christou, G. *Inorg. Chem.* **1997**, *36*, 109. (d) Jones, L. F.; Rajaraman, G.; Brockman, J.; Murugescu, M.; Sanudo, E. C.; Raftery, J.; Teat, S. J.; Wernsdorfer, W.; Christou, G.; Brechin, E. K.; Collison, D. *Chem.—Eur. J.* **2004**, *10*, 5180.

(34) Kambe, K. *J. Phys. Soc. Jpn.* **1950**, *5*, 48.

(35) (a) Brechin, E. K.; Sanudo, E. C.; Wernsdorfer, W.; Boskovic, C.; Yoo, J.; Hendrickson, D. N.; Yamaguchi, A.; Ishimoto, H.; Concolino, T. E.; Rheingold, A. L.; Christou, G. *Inorg. Chem.* **2005**, *44*, 502.

(b) Stamatatos, Th. C.; Luisi, B. S.; Moulton, B.; Christou, G. *Inorg. Chem.* **2008**, *47*, 1134. (c) Sanudo, E. C.; Wernsdorfer, W.; Abboud, K. A.; Christou, G. *Inorg. Chem.* **2004**, *43*, 4137. (d) Tasiopoulos, A. J.; Wernsdorfer, W.; Abboud, K. A.; Christou, G. *Inorg. Chem.* **2005**, *44*, 6324. (e) Murugesu, M.; Raftery, J.; Wernsdorfer, W.; Christou, G.; Brechin, E. K. *Inorg. Chem.* **2004**, *43*, 4203.